The electron and energy transfer between oligothiophenes and thieno[3,4-*b*]thiophene units

Jodi Szarko[§,△], Jianchang Guo[△,○], Yongye Liang[○], Brian Rolczynski[§,△], Luping Yu[○] and Lin X. Chen[§,△,*]

§ *Department of Chemistry, Northwestern University, Evanston, Illinois 60208*
△ *Chemical Sciences and Engineering Division, Argonne National Laboratory, Argonne, Illinois 60439*
○ *Department of Chemistry, University of Chicago, Chicago, Illinois, 60637*

ABSTRACT

In a recent study, it has been shown that organic photovoltaic (OPV) solar cells consisting of polymers with certain stoichiometric ratios of alkyl thiophene:thieno[3,4-*b*]thiophene monomeric units in random sequences, when combined with [6,6]-phenyl-C_{61}-butyric acid methyl ester (PCBM), may have potentials for creating more efficient devices. Such a potential enhancement is mainly due to the light harvesting in most of the visible and near infrared region by these low band-gap polymers. However, very little is known about the photoinduced energy/electron transfer and transport within these copolymers. It is important to understand both the ultrafast interactions between these two monomeric units when they are linked in the copolymers and their interactions with the electron acceptor PCBM in order to determine the transport mechanisms in these systems, and then to create the architectures that optimize electronic transport properties. Therefore, three oligomer molecules have been synthesized to model the local interactions in the copolymers, each of which consists of a thieno[3,4-*b*] thiophene derivative at its center linked with two alkyl oligothiophene side units. The alkyl oligothiophene units for the three molecules are 2, 4, or 8 units in length. By performing transient absorption and fluorescence upconversion measurements, the nature of the early exciton diffusion and energy transfer between these different units is elucidated.

Keywords: oligothiophene, thienothiophene, transient absorption, fluorescence upconversion

1. INTRODUCTION

Since the discovery of photoconducting polymers, there has been an increasing interest in improving and modifying the building blocks of these structures to make more efficient, durable materials for various applications.[1] Photoconducting polymers can be used in devices such as organic light emitting diodes (OLEDs) and organic photovoltaic (OPV) cells. In OPV cells, derivatives of polythiophene are often used as the electron donor while the electron acceptor is typically a molecule such as PCBM.[2] Polythiophene derivatives have shown great potential as hole conductors because of their electronic and structural properties. The π-conjugation along the polymer chain between monomeric units allows for the effective transport of electrons and holes through the polymer backbone. The chains are also sufficiently stable in air, and several derivatives have been widely produced, such as poly-3-hexathiophene (P3HT).[3-5] One of the drawbacks of the polythiophene or P3HT in photovoltaic operations is the lack of capability of harvesting photons in the red and near infrared spectral regions, where there is a substantial portion of the solar photon flux, because the bandgap of P3HT is higher in energy.[6,7] Therefore, much effort has been put into making polymers with lower bandgaps by adding units with larger range of π-conjugation.[8] Polythieno[3,4-*b*] thiophene has been synthesized recently as a conducting polymer with a bandgap as low as 0.85 eV.[9] One of the main mechanisms for the lowering of the bandgap is the increased quinoidal character of the system relative to its simpler polythiophene counterparts.[10] Although the films would be used in OPV devices, it is important to establish correlations between electronic properties, such as fluorescence lifetimes, spin-orbit coupling, ionization potentials, and electronic relaxation lifetimes, with structures of the monomer and polymer for understanding the nature of electron and charge transport in these systems and synthesizing polymers with targeted properties.

* email:lchen@anl.gov

Physical Chemistry of Interfaces and Nanomaterials VII, edited by Garry Rumbles, Oliver L. A. Monti, Proc. of SPIE Vol. 7034, 703403, (2008) · 0277-786X/08/$18 · doi: 10.1117/12.797442

A thieno[3,4-*b*]thiophene derivative containing an ester group in the 2- position has recently been produced.[11] This ester group has two functions: the electron withdrawing nature of the oxygen-rich ester stabilizes the HOMO level of the thienothiophene while its bulky alkyl group enhances the solubility of the molecule for polymer synthesis. This molecule, when attached to a single thiophene unit, was polymerized to give a low bandgap conducting polymer. The bandgap of the copolymer can be chemically tuned via varying the ratio of thiophene:thieno[3,4-*b*]thiophene monomeric units. We have shown very recently that combining these copolymers with PCBM in the film gives reasonable solar cell efficiencies.[12] In the model oligomer series, there is a systematic increase of the bandgap as the number of thiophene units is increased. When the ratio of the thiophene units to the thienothiophene units is sufficiently high (i.e., 8:1), the characteristics of the copolymer start to closely resemble those of P3HT. To better understand the underlying characteristics that determine the solar cell efficiencies, we first studied the monomeric units because they are structurally well defined. We hope to use these models to gain further insight into the nature of charge and electron transfer between the thiophene and thienothiophene units in the low-bandgap copolymers. This study will compare the initial electron transport mechanisms of these molecules to the more conventionally used oligothiophene species, which have been studied extensively, and will also explore the applications with sequence specific oligomers as OPV materials.[13-22] Three model oligomers are studied which have basic structures shown in Figure 1, and are denoted to M5, M9, and M17 with a central thieno[3,4-*b*] thiophene units attached to 2, 4, or 8 thiophene units on both sides, respectively.

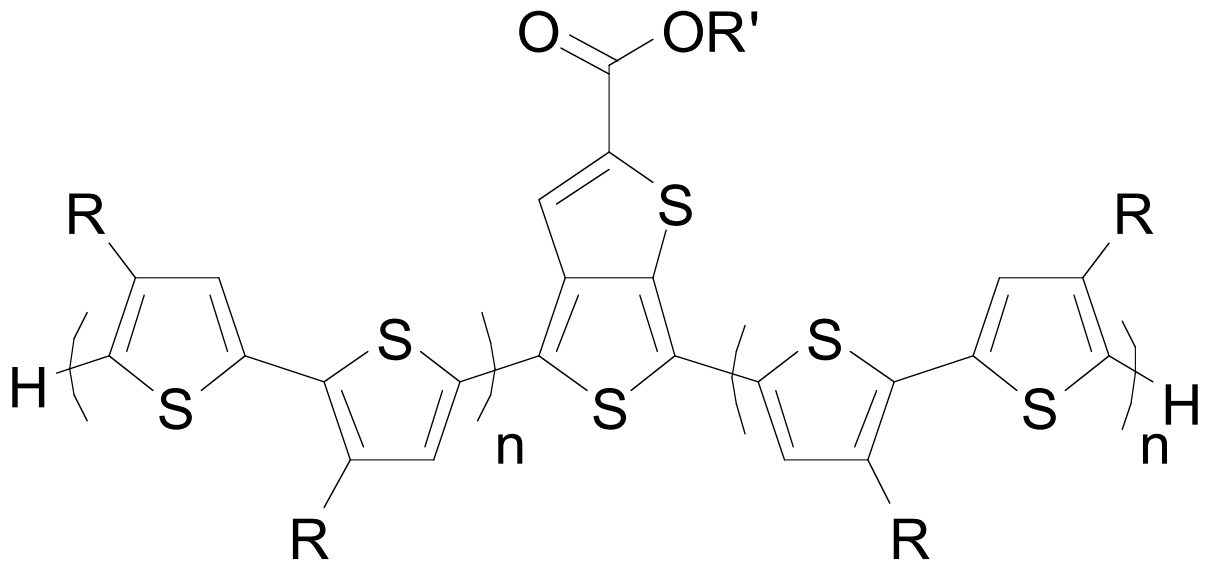

Figure 1. Basic structure of the M5, M9, and M17 molecules. The R group is n-hexane while the R' group is 2-methyltetradecane. For M5, n=1, for M9, n=2, and for M17 n=4.

The steady-state absorption, fluorescence, transient absorption, and fluorescence upconversion signals were measured in toluene solutions. These experiments were performed to gain insight on the radiative and nonradiaitve lifetimes and the intersystem crossing of the singlet-triplet states. These findings, when compared to similar experiments performed on thin films both with and without PCBM, will give further insight into the electron transport mechanisms involved in these devices.

2. EXPERIMENT

The synthesis of M5, M9 and M17 will be described elsewhere.[23] The molecular concentrations were measured in a toluene solution and were estimated to be ~10^{-4} - 10^{-5} M. Changing the concentration of the solutions did not affect the steady state absorption and fluorescence spectra, indicating that effects of aggregation are minimal. The absorption and

fluorescence spectra were obtained using a Shimadzu UV-2401PC recording spectrophotometer or a Shimadzu UV-1609 spectrophotometer and by a PTI Fluorescence Master Series fluoremeter or a Shimadzu RF-5301PC spectrofluorophotometer, respectively.

Two ultrafast transient absorption spectroscopy setups were used. For the transient absorption spectra, a home-built 1KHz regenerative amplified laser system operating at 806 nm was used. A major fraction of the light was frequency doubled to produce the 403 nm pump beam while a minor portion of the light was focused into a 2 mm sapphire plate to create a white light continuum (wlc). The response function of the system was roughly 180 fs. The kinetics and spectral signals were obtained using a differential detection technique and acquired using a home-built software package.

For the fluorescence upconversion measurements, a 100-250 kHz Coherent RegA system centered at 790 nm was used. Part of the light was frequency doubled to create the 395 nm pump light while another portion of the light was used as the 795 nm gate pulse. Both the 395 nm and 795 nm beams were directed into the Ultrafast System Halcyone fluorescence setup. The 790 nm beam was directed to a retroreflector attached to a variable translation stage. The 395 nm light was focused into a 2 mm cuvette containing the solutions studied. The solutions were stirred using a small magnetic stirrer to minimize effects such as heating and sample degradation. The solution samples were studied within a few hours of after they were dissolved. The fluorescence signals passed through a longpass filter with a 420 nm cutoff. The fluorescence light and the 790 nm light were then focused onto a BBO crystal cut to optimize the sum frequency generation (SFG) of the signal. The SFG signals were created when the fluorescence and gate pulses were combined in the crystals, and were directed into a monochromator and single photon counting PMT setup. The instrument response function was less than 500 fs. The kinetics traces were obtained by varying the time delay between the excitation pulse and the gate pulse through moving the variable translation stage connected with the gate pulse. The detection wavelengths were changed using the monochromator. Since the efficiency of the SFG changes as a function of the wavelength, the crystal angle is optimized for each kinetics trace at the different wavelengths.

3. RESULTS AND DISCUSSION

3.1 Steady-state spectra

The steady-state absorption and emission spectra are shown in Fig. 2 for the M5, M9, and M17 molecule in toluene solutions. Two main peaks are observed in the absorption spectra., which are assigned to the $S_2 \leftarrow S_0$ and the $S_1 \leftarrow S_0$ transitions. These peaks were roughly fit to a Gaussian and give maxima at 377 nm and 498 nm for M5, 397 nm and 528 nm for M9, and 425 and 535 nm for M17. Although it is not shown, the spectra in chlorobenzene were also investigated. No wavelength shift of these peaks is observed, but the intensity of the higher energy peak relative to the lower energy peak increases in chlorobenzene compared to toluene. The absorption cross sections of the molecules in toluene are 30,000 M^{-1} cm^{-1} for the M5 and M9 molecules at λ_{max} while the cross sections for the M17 molecule are 36,000 M^{-1} cm^{-1} at 535 nm and 52,000 M^{-1} cm^{-1} at 425 nm. The fluorescence quantum yields were compared to a Zinc tetraphenylporphyrin (ZnTPP) standard and give values of 0.16, 0.08 and 0.08, respectively. The maxima of the fluorescence curves are at 597 nm for M5, 637 nm for M9, and 643 nm for M17. The apparent Stokes shift obtained from these experiments is 3330 cm^{-1} for M5, 3240 cm^{-1} for M9, and 3139 cm^{-1} for M17.

The observed spectra show a decrease in the absorption onset compared to thiophene oligomers that do not contain a fused ring.[17,19] The copolymerization of various quinoidal units such as thieno[3,4-*b*]pyrazine and isothianaphthene with aromatic units such as thiophene have been utilized to decrease the bandgap of conducting polymers.[1] The bandgap decreases due to the quinoidal nature of the fused fragments. It has been established both theoretically and experimentally that the quinoidal and aromatic states of thieno[3,4-*b*]thiophene are nearly equal in energy.[24,25] Therefore, the bandgap of the polymerized form of this unit is lower than that of pure thiophene, but higher than the bandgap of more quinoidal units such as isothianaphthene. The estimated bandgap is 1.5 eV, which is ideal for solar cell applications.[7] In these experiments, a red shift of both the $S_1 \leftarrow S_0$ transition and the $S_2 \leftarrow S_0$ transition is observed as the molecular length increases. This suggests that the delocalization of the excited state electron increases with size. For conjugated oligomer systems, there is typically a linear relationship between the electronic transition energy and the inverse number of monomer units in the system.[17] The molecules here slightly deviate from a line, which suggests some saturation of the chain length in the longest molecule. The initial molecular orbital picture was investigated using the ZINDO/S method in Hyperchem. The red shift of the two lowest transitions is mimicked in these calculations. The

molecular orbital picture also shows the delocalization of the electron along the thiophene chain. The lowest unoccupied molecular orbital (LUMO) for the M17 molecule only extends through the nine center units while the highest occupied molecular orbital (HOMO) extends through the whole molecule. The LUMOs and HOMOs for M9 and M5 extend over the entire molecule. The first and second allowed transitions for the molecules also have increased configuration interaction (CI) contributions from orbitals other than the HOMO as the molecule increases, which is common as the number of orbitals increases.[26]

The absorption coefficients increase as the molecular unit increases, which indicates an increase in the transition moment as the conjugation of the molecule is extended. An increase in the oscillator strengths as the molecules increase is also shown in the Hyperchem calculations. The quantum yield for unsubstituted thiophene oligomers and P3HT of similar length typically show quantum yields of 30-40%[14,27] while oligomers such as hexamethylsexithiophene have shown quantum yields of 10%.[28] The structure of the fluorescence spectra does not show any obvious vibronic character. Similar behavior has also been observed in the hexamethylsexithiophene oligomer.[29] The large Stokes shift and vibrational broadening most likely have contributions from conformational shifts between the excited and ground states and the spectral diffusion caused by the differences in local potential wells within the polymer backbone. This point will be discussed in more detail in the Section 3.3.

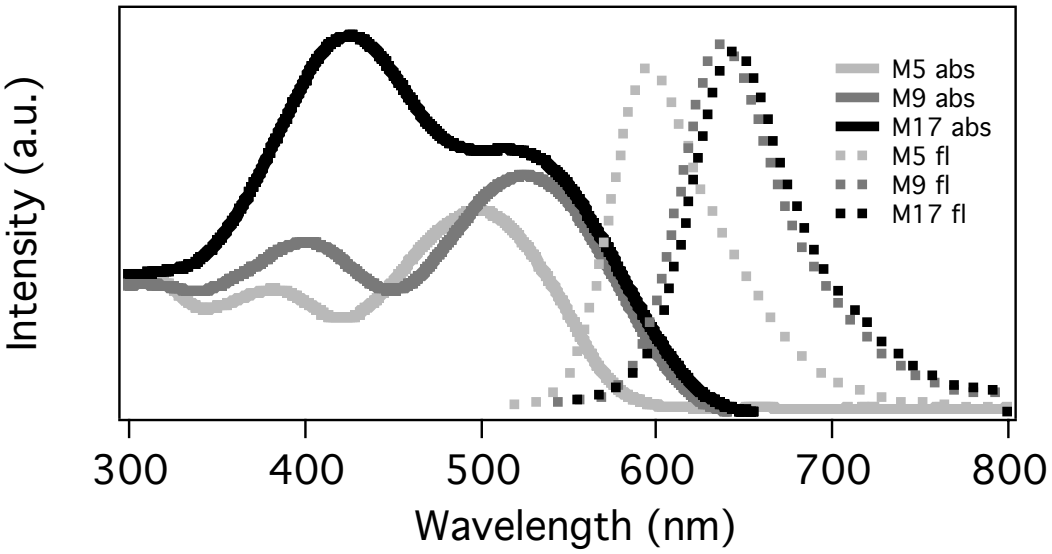

Figure 2. The absorption spectra (solid lines, denoted abs) and fluorescence spectra (dashed lines, denoted fl) of the 3 molecules studied in this work in a toluene solution.

3.2 Transient absorption spectra

The transient absorption spectra for M5 and M9 in toluene are shown in Fig. 3 using a 403 nm pump pulse. The transient signals for M17 and M9 are very similar and therefore the spectrum for M17 is not shown for clarity. In Fig. 3 (left side), two main peaks are clearly present for the M5 transient absorption spectra. The isosbestic point for transient spectra between 3 ps and 500 ps is at 682 nm. For the spectra in between 500 ps and 2 ns, the isosbestic point is shifted to 686 nm, which indicates that a third species, such as the stimulated emission from the S_1 state, slightly obscures the transient absorption signals. Compared to the oligothiophene, the isosbestic point is red shifted about 30 nm,[30] but the general spectral characteristics are the same. The two main features in this region are dominated by the decay of the singlet excited state and the rise of an exited triplet state. The singlet-triplet intersystem crossing rates in thiophene units have been studied extensively. It has been shown that oligothiophenes containing two thiophene units show the strongest spin-orbit interaction, which gives rise to fast singlet-triplet relaxation times of less than 100 ps.[14,31] At early times (before 500 ps), the stimulated emission is also observed as a negative signal from 550-650 nm. Therefore, the increase in the absorption of the triplet state and the decrease of the stimulated emission from the first singlet excited state are

represented in Fig. 3 (left side). A small negative signal is observed at 500 nm and is attributed to the ground state bleaching of the molecule. This signal does not vary much over the entire temporal range of the experiment, which indicates that the molecule has a much longer triplet state lifetime than 2 ns. The lifetime of the triplet state in similar systems is typically on the order of tens of microseconds or longer.[14] When looking at the M9 spectra (Fig. 3, right side), the isosbestic region is not observed due to the red shift of the excited singlet and triplet states. The same general trends are observed in the M9 spectra and the M5 spectra, namely a) the decrease of signal in the near infrared region due to $S_1 \rightarrow S_N$ absorption which represent the singlet excited state of the molecule, b) the triplet-triplet absorption starting at 600 nm which represents the formation of the triplet state from the singlet state by intersystem crossing, which is very long-lived, and c) the two negative peaks at early times which represent the stimulated emission and ground state bleaching of the sample.

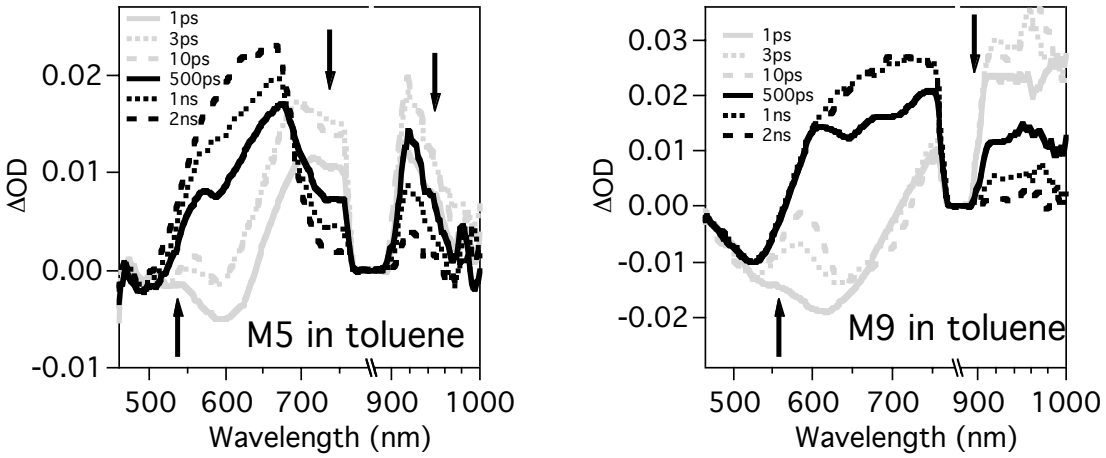

Figure 3. The transient absorption spectra of M5 (left) and M9 (right) in a toluene solution. The pump wavelength for these spectra was 400 nm. The arrows indicate the increase or the decrease on the signals in time for a given spectral region. The lack of signal around 800 nm is due to the filtering of the high intensity 800 nm light.

The kinetics traces of the molecules are shown in Fig. 4. In the near infrared region, the kinetic signals at 930 nm for M9 and M17, which originate from the excited state absorption, are remarkably similar. The signal for M9 shows a monoexponential decay curve with a lifetime of 550 ps, whereas that for M17 is slightly biexponential with time constants of 17 ps and 540 ps. For the M5 molecule, the kinetics signal fits to a multiexponential function with a rise time of 9 ps and a decay time of 1 ns. When looking at the rise time signal at shorter wavelengths, the kinetic curves appear to represent the lifetime of several processes in the sample. Although it is not shown, the kinetics traces of M9 at 725 nm and 630 nm were compared. At 725 nm, an initial absorption is observed followed by the rise of the stimulated emission signal. At longer times, the rise of the triplet excited state absorption signal in conjunction with the decay of the stimulated emission signal give rise to an increase of the excited state absorption as a function of time. At 630 nm, an instantaneous emission is observed. Several time constants are needed to fit the rise of the absorption signal, which adds error to the numerical validity of the decay times obtained, but they can still give rise to a general trend of the kinetics in this region. A fast 10 ps decay of the stimulated emission is observed, which is followed by a rise of the absorption spectrum. The fact that the stimulated emission signal rises at 725 nm and decays at 630 nm indicates that this is the relaxation time for this molecule in the excited state. This point will be discussed further in Section 3.3. The rise time of the triplet state for both the M9 and M17 are both on the order of 330-350 ps. The rise time of the triplet state for M5 is roughly 1.2 ns. It appears as though there is a discrepancy in the rise time of the triplet excited state and the decay time of the first singlet excited state. This discrepancy is not fully understood and will be investigated further in future work. As was mentioned previously, the fact that multiple signals are present can add to the error of the lifetimes obtained in these measurements. Therefore, the fluorescence upconversion signals at comparable wavelengths will give a direct comparison of the fluorescence lifetimes since they are not obscured by the various possible absorption signals in the medium.

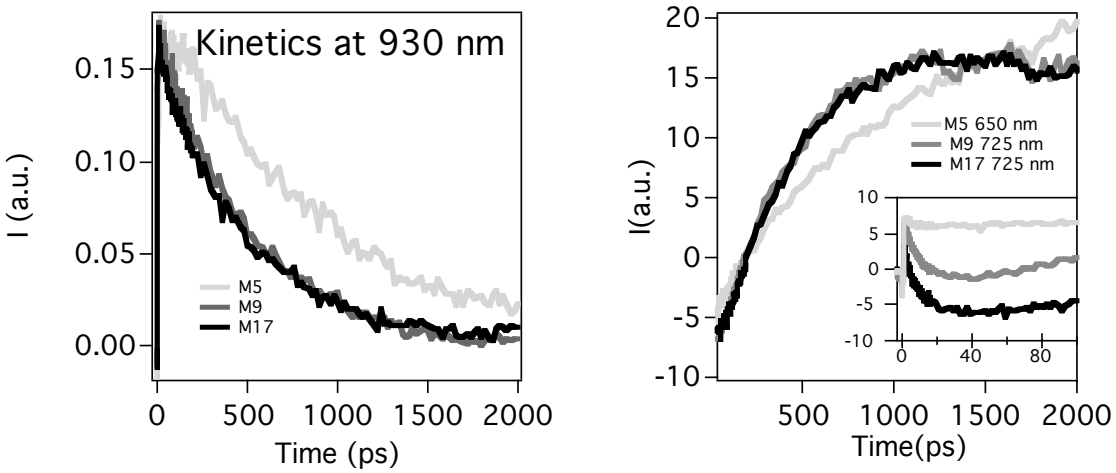

Figure 4. The kinetic traces of M5, M9, and M17. The pump wavelength for these spectra was 400 nm. The graph on the left shows the kinetics traces of all three molecules at 930 nm while the graph on the right shows the kinetics traces at 650 nm for M5 and 725 nm for M9 and M17. The difference in the wavelength for these traces was chosen to represent the spectral shifts in the emission and triplet state spectra as the molecule chain length increases. In the inset of the figure on the right, the same traces are shown at early times to better show the faster kinetics of these signals. At 930 nm, the traces represent the decay of the first excited state. At shorter wavelengths, the signals represent three main phenomena: a) the rise of the triplet state b) the decay of the stimulated emission of the first excited state, and c) the vibrational and solution facilitated relaxation of the first excited state and spectral diffusion to lower energy levels. The full scale graph on the right depicts the rise of the triplet state (a) and decay of the stimulated emission (b) while the inset depicts the relaxation and diffusion to lower energy levels (c).

3.3 Fluorescence upconversion

The wavelength dependent kinetics traces for the M9 molecule are shown in Figure 5. Once again, only the M9

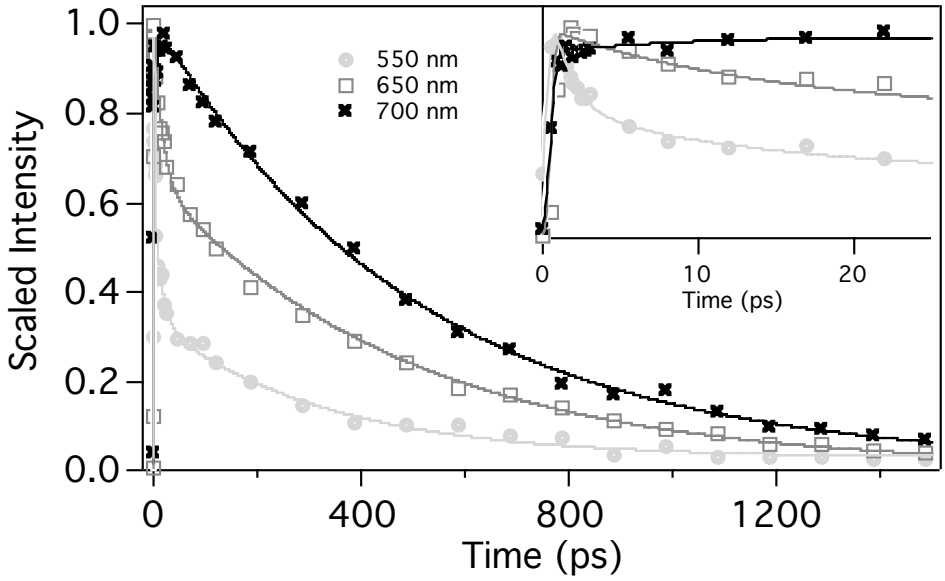

Figure 5. The fluorescence upconversion signals of M9 in a toluene solution. The pump wavelength was 395 nm. The marked points on the figure represent the experimental points while the lines represent the fit traces of the experimental data. The inset shows the same traces on a shorter time scale.

molecule is shown as an example of the wavelength dependent kinetics for clarity, but all three molecules show the same basic trends. The M17 and M9 traces are more similar than the M5 kinetics traces. The kinetics signals for the M9 and

M17 molecules were taken at 3 different wavelengths: 550 nm, 650 nm, and 700 nm. The 650 nm peak corresponds to the fluorescence maximum (Fig. 2). The 550 nm and 700 nm signals were recorded to investigate the higher and lower energy kinetics, respectively, within the fluorescence spectrum. The M5 molecule shows a blue shifted steady-state fluorescence, so the kinetics for M5 was recorded at 500 nm, 600 nm, and 650 nm. These traces were fit to a biexponential or triexponential decay. It is not currently fully understood why a triexponential fit is needed to fit the 550 nm traces for M9 and M17, but this point will be further investigated. Table 1 shows the time constants from these fits. These results show that the fluorescence lifetime for these molecules in the blue shifted region decreases with the chain length. The fluorescence is too high to be from an $S_2 \rightarrow S_1$ transition, so it is believed that this signal comes from the emission of the first excited state to the ground state before electronic relaxation. The faster decay time of at 650 nm and the rise time at 700 nm are ascribed to a relaxation process in the molecule and is slower for the M17 molecule. The 490-500 ps decay is assigned mainly to the intersystem crossing in the systems.

molecule	λ(nm)	A1	τ_1 (ps)	A2	τ_2(ps)	A3	τ_3 (ps)
M5	500	-	-	0.48	10	0.34	560
	600	-	-	.20	4.4	.74	640
	650	-	-	-0.10	1.9	0.92	700
M9	550	.57	1.3	.28	13	.30	320
	650	-	-	.33	16	.64	490
	700	-	-	-0.12	12	.99	500
M17	550	1.0	.6	.4	6.1	.12	260
	650	-	-	.28	18	.65	490
	700			-0.18	21	1.0	500

Table 1. The biexponential and triexponential fits of the fluorescence upconversion signals for the M5, M9, and M17 molecules at various wavelengths. A1, A2, and A3 are the amplitudes of the time constants τ_1, τ_2, and τ_3, respectively.

The kinetics spectra at the low energy side of the emission spectrum for all three molecules are shown in Fig. 6. When comparing the M9 and M17 molecules, the longer kinetics traces are nearly identical. At shorter times, the M9 molecule appears to have a faster rise time. The fit of the kinetics traces for M9 at 700 nm indicates a rise time of 12 ps and a decay time of 500 ps. While the fit for the M17 molecule indicate a rise time of 21 ps and a decay time of 500 ps. In comparison to the M9 and M17 molecules, the M5 molecule has a longer fluorescence time. The kinetics trace for the M5 molecule at 650 nm shows a rise time of 2 ps and a decay time of 700 ps. It should be noted that the M5 molecule is highly sensitive to the solution environment. Although the experiments were performed within the first few hours of sample preparation and nitrogen was aerated through the sample to prevent oxygen quenching of the molecule, the signals did show some signs of degradation after about 4 hours. The decay signals obtained for M5 ranged from 700-900 ps. This relatively large range could be due to the sensitivity of the signal on the environment.

The relative radiative and nonradiative lifetimes of the signals can be extracted by the relationship $\varphi = k_r/(k_r+k_{nr}) = k_r\tau_f$.[32] As was mentioned previously, the quantum yield for M5 is 0.16 while the quantum yields for M9 and M17 are 0.08. This relationship gives radiative lifetime of roughly 4-6 ns for M5 and 6 ns for M9 and M17. The nonradiative lifetimes are 800 ps -1.2 ns for M5 and 540 ps for M9 and M17. The nonradiative decay times for M9 and M17 are similar to the decay times observed for the excited state in the transient absorption signals. The radiative decay represents the time it would take for the first excited state to relax to the ground state in the absence of any other pathways while the nonradiative rate represents the rate in which the molecule relaxes to all other pathways. For similar oligothiophenes, the nonradiative decay is dominated by the intersystem crossing rate between the first excited state and the triplet state. The triplet coupling is greatest in bithiophene units and is dominated by the $S_1 \rightarrow T_4$ transition, where the molecule then undergoes rapid relaxation into the T_1 state.[33] It was also established theoretically that adding electron donor or acceptor groups to the oligomer did not change the inter system crossing rate significantly. Fluorescence lifetime studies on alpha thiophenes have shown a lifetime of 46 ps for the bithiophene oligomer.[14] This lifetime increases to 970 ps for the hexathiophene oligomer and plateaus for the longer oligomers. Here the nonradiative decay times decrease with as the chain length increases, which would typically indicate an increase in the delocalization of the electron in the molecule. For the molecules investigated in these experiments, the decay times are similar to the maximum fluorescence lifetime obtained for the alpha oligothiophenes. Therefore, it is assumed that the fluorescence lifetimes are dominated by the nonradiative decay into the T_4 state, but the decrease in the fluorescence lifetimes with increasing chain length show that

other nonradiative pathways have a larger effect as the molecule size increases. Finally, the similarity in both the quantum yield values and excited state decay lifetimes for the M9 and M17 molecules indicate that the effective chain length most likely reaches a saturation point close to the length of the M9 molecule, which is also indicated by the LUMO of the M17 molecule obtained from the molecular orbital calculations mentioned previously.

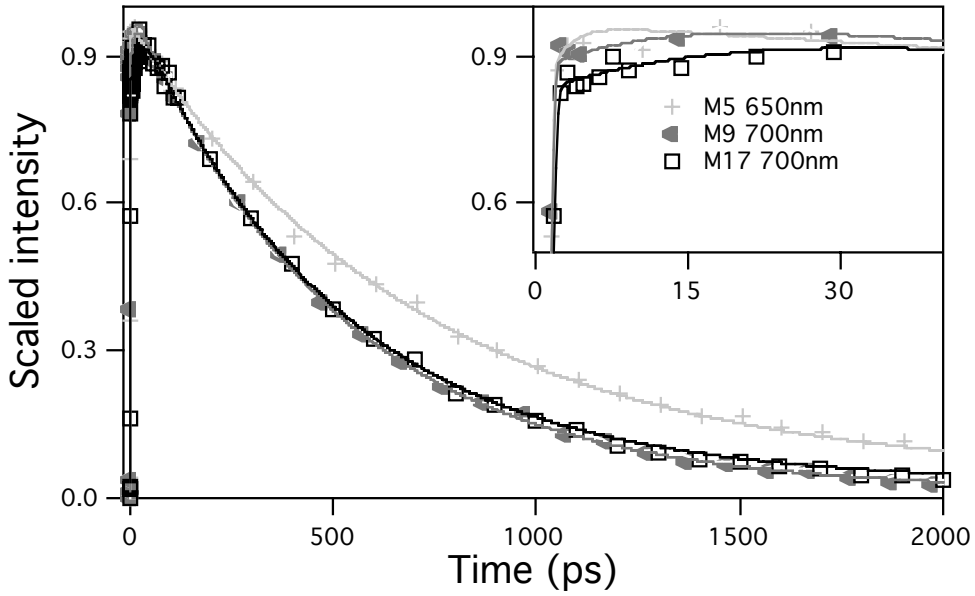

Figure 6. The low energy fluorescence upconversion signals in M5, M9, and M17. The pump wavelength was 395 nm. The markers represent experimental data points and the lines represent the fit traces of these points. The inset shows the same traces on a shorter time scale.

Although the fluorescence lifetime gives very important information about the electronic characteristics of these molecules, the time range in which the electron relaxes from the S_1 state is not expected to have a very significant effect on the overall solar cell efficiency. The intersystem crossing rates would have a large effect on the efficiency of OLED devices. When blended with PCBM, electron donating polymers typically exhibit a sub-picosecond electron transfer into the PCBM molecule.[34,35] The conformational and vibrational relaxation of the polymers, which are in the ps regime, could effect the electron transfer into the PCBM moiety. The relaxation of the excited state towards lower energies increases with the molecule size. For the M17 molecule, the energy relaxation lifetime is 20 ps, which is considerably long-lived for a purely vibrational relaxation. These time scales indicate that the molecules undergo spectral diffusion of the excitons.[36] As the exciton, which travels through the backbone of the oligomer, interacts with local barriers within the chain, the excitons become trapped the lowest energy levels. Such behavior is also observed in random thiophene copolymers[37] and poly(3-octyl)thiophene.[38] It is interesting to note that the higher energy decay time of the molecules decrease with chain length while the low energy rise time increase with chain length. Conformational changes in the molecular chain will create lower energy pathways for the excitons to relax.[38] The change in the structure will effect the hole mobility in these systems. The solvent relaxation effect also plays a role in the long term reorganization of these molecules, so it is necessary to compare these results with thin film samples. Performing solvent dependent and polarization anisotropy experiments will help us to further characterize the relaxation mechanisms in these molecules.

4. CONCLUSIONS

In this work, we have determined the excited state lifetime of three thieno[3,4-*b*]thiophene-thiophene oligomers to model the excited state dynamics of a group of low band gap polymers that show promising potential in enhancing the efficiency of solar cells when they form composite with PCBM in films. The main features of the transient absorption are the decay of the first excited state, the rise of the triplet state, and the decay of the stimulated emission. The conformational relaxation of the excited state is also observed, but it is obscured by the other signals. The first excited state for these molecules decays in less than one nanosecond for all molecules and is due to the intersystem crossing into

an excited triplet state. These molecules also exhibit a chain length dependent relaxation time, which will affect the electron transfer mechanism into electron acceptor moieties. These experiments have facilitated in the basic understanding of energy and charge transfer in these systems. By combining these experimental results with structural data, thin film experiments, and solution dependent experiments, we will better understand the nature of electron transport in these systems.

5. ACKNOWLEDGEMENTS

This work is supported by the Division of Chemical Sciences, Office of Basic Energy Sciences, the U. S. Department of Energy under contract DE-AC02-06CH11357 (for L. X. C.). We gratefully acknowledge the financial supports of the National Science Foundation and the NSF MRSEC program at the University of Chicago. The UC/ANL collaborative seed grant (L. Y. and L. X. C.) and the Setup fund from Northwestern University (L. X. C.) provided partial support of this research. The authors would also like to thank Jenny Lockard for helpful discussions and Chunxing She for assistance with the steady-state fluorescence measurements.

6. REFERENCES

[1] Skotheim, T. A. and Reynolds, J. R. [Handbook of Conducting Polymers], CRC Press, Boca Raton, 2007.
[2] Günes, S., Neugebauer, H., and Sariciftci, N.S. "Conjugated polymer-based organic solar cells." Chem. Rev., 107(4), 1324-1338 (2007).
[3] Heffner, G.W. and Pearson, D.S. "Molecular characterization of poly(3-hexylthiophene)." Macromolecules, 24(23), 6295-6299 (1991).
[4] Reyes-Reyes, M., Kim, K., and Carroll, D.L. "High-Efficiency photovoltaic devices based on annealed poly (3-hexylthiophene) and 1-(3-methoxycarbonyl)-propyl-1-phenyl-(6, 6) C_{61} blends." Appl. Phys. Lett. 87(8), 083506 (2005).
[5] Sirringhaus, H., Brown, P.J., Friend, R.H., Nielsen, M.M., *et al.* "Two-Dimensional charge transport in self-organized, high-mobility conjugated polymers." Nature, 401(6754), 685-688 (1999).
[6] Bundgaard, E. and Krebs, F. "Low band gap polymers for organic photovoltaics." Sol. Energ. Mat. Sol. C, 91(11), 954-985 (2007).
[7] Scharber, M., Mühlbacher, D., Koppe, M., Denk, P., *et al.* "Design rules for donors in bulk-heterojunction solar cells-towards 10% energy-conversion efficiency." Adv. Mater., 18(6), 789-794 (2006).
[8] Mühlbacher, D., Scharber, M., Morana, M., Zhu, Z., *et al.* "High photovoltaic performance of a low-bandgap polymer." Adv. Mater., 18(21), 2884-2889 (2006).
[9] Sotzing, G.A. and Lee, K.H. "Poly(thieno[3,4-*b*]thiophene): A p- and n-dopable polythiophene exhibiting high optical transparency in the semiconducting state." Macromolecules, 35(19), 7281-7286 (2002).
[10] Brédas, J.L., Heeger, A.J., and Wudl, F. "Towards organic polymers with very small intrinsic band-gaps .1. Electronic-Structure of polyisothianaphthene and derivatives." J. Chem. Phys., 85(8), 4673-4678 (1986).
[11] Yao, Y., Liang, Y., Shrotriya, V., Xiao, S., *et al.* "Plastic near-infrared photodetectors utilizing low band gap polymer." Adv. Mater., 19(22), 3979-3983 (2007).
[12] Liang, Y., Xiao, S., Feng, D., and Yu, L. "Control in energy levels of conjugated polymers for photovoltaic application." J. Phys. Chem. C, 112(21), 7866-7871 (2008).
[13] Anestopoulos, D., Fakis, M., Polyzos, I., Tsigaridas, G., *et al.* "Time-Resolved spectroscopy of oligothiophenes using the femtosecond fluorescence upconversion technique." J. Phys.: Conf. Ser., 10(1), 230-233 (2005).
[14] Becker, R.S., deMelo, J.S., Macanita, A.L., and Elisei, F. "Comprehensive evaluation of the absorption, photophysical, energy transfer, structural, and theoretical properties of alpha-oligothiophenes with one to seven rings." J. Phys. Chem., 100(48), 18683-18695 (1996).
[15] Sugita, A., Shiraishi, Y., and Kobayashi, T. "Femtosecond-Picosecond dynamics of the lowest excited singlet state in alpha-quinquethiophene." Chem. Phys. Lett., 296(3-4), 365-371 (1998).
[16] Helbig, M., Ruseckas, A., Grage, M.M.L., Birckner, E., *et al.* "Resolving the radical cation formation from the lowest-excited singlet (S_1) state of terthiophene in a TiO_2-SiO_2 hybrid polymer matrix." Chem. Phys. Lett., 302(5-6), 587-594 (1999).
[17] Izumi, T., Kobashi, S., Takimiya, K., Aso, Y., and Otsubo, T. "Synthesis and spectroscopic properties of a series of beta-blocked long oligothiophenes up to the 96-mer: Revaluation of effective conjugation length." J. Am. Chem. Soc., 125(18), 5286-5287 (2003).

[18] Lanzani, G., Nisoli, M., Desilvestri, S., and Tubino, R. "Femtosecond vibrational and torsional energy redistribution in photoexcited oligothiophenes." Chem. Phys. Lett., 251(5-6), 339-345 (1996).
[19] Yang, A., Kuroda, M., Shiraishi, Y., and Kobayashi, T. "Chain-length dependent stationary and time-resolved spectra of alpha-oligothiophenes." J. Phys. Chem. B, 102(19), 3706-3711 (1998).
[20] Nakamura, T., Araki, Y., Ito, O., Takimiya, K., and Otsubo, T. "Fluorescence up-conversion study of excitation energy transport dynamics in oligothiophene-fullerene linked dyads." J. Phys. Chem. A, 112(6), 1125-1132 (2008).
[21] Benincori, T., Bongiovanni, G., Botta, C., Cerullo, G., *et al.* "Tuning of the excited-state lifetime by control of the structural relaxation in oligothiophenes." Phys. Rev. B, 58(14), 9082-9086 (1998).
[22] Chosrovian, H., Rentsch, S., Grebner, D., Dahm, D.U., *et al.* "Time-Resolved fluorescence studies on thiophene oligomers in solution." Synth. Met., 60(1), 23-26 (1993).
[23] Liang,Y. and Yu, L., publication in progress.
[24] Hong, S.Y. and Marynick, D.S. "Understanding the conformational stability and electronic structures of modified polymers based on polythiophene." Macromolecules, 25(18), 4652-4657 (1992).
[25] Pomerantz, M., Gu, X.M., and Zhang, S.X. "Poly(2-decylthieno[3,4-*b*]thiophene-4,6-diyl). A new low band gap conducting polymer." Macromolecules, 34, 1817-1822 (2001).
[26] Cornil, J., Beljonne, D., and Brédas, J.L. "Nature of optical transitions in conjugated oligomers. Ii. Theoretical characterization of neutral and doped oligothiophenes." J. Chem. Phys., 103(2), 842 (1995).
[27] Magnani, L., Rumbles, G., Samuel, I.D.W., Murray, K., *et al.* "Photoluminescence studies of chain interactions in electroluminescent polymers." Synth. Met., 84(1-3), 899-900 (1997).
[28] Lanzani, G., Nisoli, M., De Silvestri S, Barbarella, G., *et al.* "Visible and near-infrared ultrafast optical dynamics of hexamethylsexithiophene in solution." Phys. Rev. B, 53(8), 4453-4457 (1996).
[29] Wong, K.S., Wang, H., and Lanzani, G. "Ultrafast excited-state planarization of the hexamethylsexithiophene oligomer studied by femtosecond time-resolved photoluminescence." Chem. Phys. Lett., 288(1), 59-64 (1998).
[30] Rentsch, S., Yang, J., Paa, W., Birckner, E., and Scheidt, J. "Size dependence of triplet and singlet states of α-oligothiophenes." PCCP, 1(8), 1707-1714 (1999).
[31] Paa, W., Yang, J.P., and Rentsch, S. "Intersystem crossing in oligothiophenes studied by fs time-resolved spectroscopy." Appl. Phys. B, 71(3), 443-449 (2000).
[32] Rumbles, G., Samuel, I.D.W., Magnani, L., Murray, K.A., *et al.* "Chromism and luminescence in regioregular poly(3-dodecylthiophene)." Synth. Met., 76(1-3), 47-51 (1996).
[33] Beljonne, D., Cornil, J., Friend, R.H., Janssen, R.A.J., and Brédas, J.L. "Influence of chain length and derivatization on the lowest singlet and triplet states and intersystem crossing in oligothiophenes." J. Am. Chem. Soc., 118(27), 6453-6461 (1996).
[34] Sariciftci, N.S., Smilowitz, L., Heeger, A.J., and Wudl, F. "Photoinduced electron-transfer from a conducting polymer to buckminsterfullerene." Science, 258(5087), 1474-1476 (1992).
[35] Lioudakis, E., Othonos, A., Alexandrou, I., and Hayashi, Y. "Ultrafast carrier dynamics on conjugated poly(3-hexylthiophene)/[6,6]-phenylC_{61}-butyric acid methyl ester composites." Appl. Phys. Lett., 91(11), 111117 (2007).
[36] Chen, L.X., Jäger, W.J.H., Niemczyk, M.P., and Wasielewski, M.R. "Effects of-conjugation attenuation on the photophysics and exciton dynamics of poly (p-phenylenevinylene) polymers incorporating 2, 2'-bipyridines." J. Phys. Chem. A, 103(22), 4341-4351 (1999).
[37] Bongiovanni, G., Loi, M.A., Mura, A., Piaggi, A., *et al.* "Relaxation processes in thiophene-based random copolymers." Chem. Phys. Lett., 288(5-6), 749-754 (1998).
[38] Watanabe, A., Kodaira, T., and Ito, O. "Time-Resolved emission spectra of poly (3-octylthiophene): Energy migration in the π-conjugated polymer chain." Chem. Phys. Lett., 273(3-4), 227-231 (1997).